# Grasping via entanglement

**Robert Wood** ( rjwood@seas.harvard.edu )
Harvard University https://orcid.org/0000-0001-7969-038X
**Kaitlyn Becker**
Harvard University https://orcid.org/0000-0003-2650-295X
**Clark Teeple**
Harvard Univeristy
**Nicholas Charles**
Harvard University
**L. Mahadevan**
Harvard University https://orcid.org/0000-0002-5114-0519

**Physical Sciences - Article**

**Keywords:** grasping strategy, complex shapes

**Posted Date:** April 20th, 2021

**DOI:** https://doi.org/10.21203/rs.3.rs-402473/v1

# Grasping via entanglement

Kaitlyn P. Becker[1], Clark B. Teeple[1], Nicholas Charles[1], L. Mahadevan[1,2,*], Robert J. Wood[1,*]

[1]School of Engineering and Applied Sciences, Harvard University, Cambridge, MA, USA

[2]Departments of Physics, and Organismic and Evolutionary Biology, Harvard University, Cambridge, MA, USA

[*]To whom correspondence should be addressed; E-mail:

lmahadev@g.harvard.edu, rjwood@seas.harvard.edu

**We present a grasping strategy for complex shapes via the collective entanglement of and by an array of actuated filaments. The basic unit of this array is a slender hollow elastomeric filament that is pneumatically actuated to form a highly curved structure. The multiple self and mutual contact interactions between the filaments and the object create a randomly tangled spatial assemblage that enables a soft conformable grasp. We realize this using a gripper enabled by a new fabrication method to create inexpensive and modular arrays of fluidically actuated elastomeric filaments. We demonstrate that a collective of highly compliant filamentous actuators is capable of a soft, adaptable grasp across a range of loads that vary in size, shape, and geometric and topological complexity without any feedback. A theoretical framework for the collective mechanics of filaments in contact with complex objects allows us to explain our experimental findings, while a phase diagram characterizes the design space in terms of the properties of the gripper and the target. Overall, our grasping approach adapts to the mechanical, geometric, and topological complexity of target objects via an uncontrolled, spatially distributed, and heterogeneous scheme without perception or planning, in sharp contrast with current deterministic feedback-driven robotic grasping methods.**

Grasping an object securely typically requires some knowledge of its size, shape, and mechanical properties. This is done, seemingly without effort, by elephants whose trunks can pick up a peanut or uproot a tree within their reach, or orangutans whose combination of reaching and grasping allows them to brachiate rapidly in a complex arboreal environment. In the engineered world of robotic grasping, inspired primarily by the remarkable dexterity of the human hand, much work has focused on understanding the mechanics, dynamics, and control of grippers as they interact with target objects (1, 2). One common approach is to study how the form and stiffness of the grasper (relative to that of the target) determines the number (topology), shape (geometry), and magnitude (mechanics) of contacts and associated stresses, while also improving the sensing of the target (3, 4). This has led to a hand-centric design paradigm (2) where robotic grippers take the form of an articulated set of locally-controlled rigid links, while also relying on an opto-motor feedback loop linking perception, planning, and action to achieve a grasping goal. Modern rigid grippers show great promise with many controllable degrees of freedom and embedded sensors (5–9), but can present challenges for grasp planning and control in the presence of uncertainty, or with complex target geometries (10, 11).

More recently, the introduction of compliant elements and under-actuated control into otherwise-rigid fingers provides a form of mechanical intelligence that drastically reduces the planning and control requirements for successful grasping. These graspers are exemplified by having a small number of degrees of freedom associated with the distal portions and a series of proximal joints that are soft and can thus allow increased adaptability of contact configurations with the target (12–16). This concept of strategic compliance is further extended in fully-soft robotic digits, utilizing soft materials throughout the entire digit structure to enable digits to conform to a wider variety of objects (17–23). Fully soft graspers circumvent precise feedback control and instead rely on mechanical deformation at multiple scales, both distally and proximally. Devolving some of the mechanical complexity of a grasping task to morphology and passive mechanics and dynamics leads to conformable contact that, even in the absence of feedback, is adaptable and robust to a range of variations in the target shape, size, and properties, and robust to damage in soft, passive, end-effectors (24–26). However, this still leaves open the question of how to grasp objects that are geometrically and topologically complex, and mechanically heterogeneous, e.g. plants, produce, fragile marine fauna, or many human-made

devices.

Here, we leverage the topological, geometrical, and mechanical flexibility afforded by slender pneumatically actuated filaments to realize a grasping strategy capable of adapting to the topological, geometric, and mechanical complexity of a range of target objects even in the absence of perception, planning, or feedback control. In this way, our grasping strategy resembles that of tentaculate entangling predator behavior of many medusae, siphonophorae, and ctenophorae (27). The basic building block of this strategy is a slender elastomeric filament with an eccentric hole running axially (sealed at one end). Filaments are made using a dip-coating technique (28). These filaments are similar to, but much larger than, recently developed micro-tentacles (29), and also operate in a manner similar to plant tendrils (30) and robotic mimics thereof (31), but are much faster owing to the rapidity of pneumatic actuation relative to growth or shrinkage driven tendrils and tendril-bots. Our dip molding methods (see SI for details) allow for cheap, easy, and uniform construction of large arrays of actuators with a high aspect ratio (up to 200:1) for compliance, sufficient length for intertwining and engaging with target objects, and a sufficiently high actuation bandwidth for grasping tasks. The configuration shown in Figure 1a and used in the experiments below uses 12 300mm long filaments distributed in a 50mm diameter circle and connected to a single pressure source, but this design can easily be modified (see Supplemental Information-SI- for further details). When an individual filament is pneumatically or hydraulically actuated, it bends because of the eccentricity of the hole, as shown in Fig. 1b. This enables an individual filament to hang straight down under ambient pressure, form a slight curve and approach nearby filaments at low pressures, and then snap into a high curvature state to form soft distributed contact zones either with a target object, itself or other filaments as it reaches its operational pressure, as shown in Fig. 1c . The operating pressure can be tuned via fabrication methods described by Becker et al. and is set to 25psi (172 kPa) in this work.

For a single filament of radius $r$, length $l$, hole radius r, hole eccentricity $\epsilon r, \epsilon \in [0, 1]$, elastic modulus $E$, in an array with a characteristic spacing $d$, actuated by a pressure $p$, the design space of the grasper made of the same filaments is spanned by the following dimensionless parameters: gripper filament areal density $\phi_G = r^2/d^2 \ll 1$, a scaled pressure $p/E$, and finally the geometric arrangement of the filaments denoted by a scalar $S$. Additionally, if we also vary the filament length, internal radius, and eccentricity, we can control $l/r, \delta, \epsilon$, and the friction

coefficient between the filament and target material. Finally, moving from terrestrial to aquatic environments, provides an additional parameter $l/l_g$, where $l_g = (Er^2/\Delta\rho g)^{1/3}$ is a gravitational length, with $\Delta\rho$ being the difference in the density between the filament material and the ambient medium. Here, we will focus primarily on varying the gripper areal density of the filaments, $\phi_G$, for simplicity, recognizing that there is a vast range of possibilities for further exploration. An object to be grasped, on the other hand, can be characterized by its size, $R_T$, the topological complexity of its branching structure, which we capture in a simplified form using its effective volumetric density, $\phi_T$, within a convex hull around the object, and finally its mass density, $\rho_T$, that determines the object weight $\rho_T R_T^3 g$. The efficacy of the gripper is a function of its topological and geometrical complexity as well as that of the target and is a function of these dimensionless parameters.

The collective behavior of a large number of curling and twisting filaments allows them to entangle with a target and thus drape, cradle, or conform to it as a function of the actuation pressure, as shown in Fig. 1d. This further enhances the ability of an actuated array to grasp complex objects without perception, planning, or feedback merely as a consequence of their geometrically-driven collective compliance. In Fig. 1d, we show both a schematic and a physical realization of how an array of such filaments can be on, around, and in a range of target objects such as spheres, cylinders, and corals, and can grasp them via collective entanglement, highly compliant individually, but capable of substantial stiffness collectively akin to a tangled lock of hair that is much stiffer than an individual strand (32). The simplest grasps, as with the sphere, bear some resemblance to traditional grasping (1), whereas higher degrees of entanglement represent a larger departure from traditional grasping. The efficacy of this collective entanglement-based grasp is evident in Fig. 1e, where we show how the array can lift a potted plant by entangling with its complex arrangements of shoots and leaves, and how it can lift a starfish from the ocean floor.

The advantages associated with using collective entanglement of structurally soft individual filaments eliminates the dependence on planning and perception prior to grasping. Simple actuation leads to robust grasping through randomly distributed soft contacts wherein no individual filament is critical, but they collectively work for greater cumulative engagement and entanglement with other filaments, the target object, or a combination of both. This strategy thus

works well in situations that are specifically challenging to traditional soft and rigid grasping strategies, e.g., in grasping of topologically complex and delicate structures ranging from fragile house plants to deep-sea corals, bottles, tubes, tools, and irregularly shaped toys. Furthermore, our strategy suggests that the notion of force closure used in deterministic grasping (3, 33) may be less relevant to entanglement and should be revisited in a probabilistic setting. In addition, the notion of static equilibrium that is necessary for stable grasping is very different for simple contacts typical of deterministic grasping compared to the present case of redundant soft distributed contacts.

We evaluate the efficacy of a grasp minimally in terms of successfully lifting and moving an object from its initial to its final position. This requires varying the initial approach and interaction with a target of varying complexity, and addressing uncertainty in both these steps. For targets, we chose a sphere, a hollow cylinder, a torus, and a branched structure (see SI for details), and for trajectories we tried three natural steps: draping from the top ("top-drape"), draping from the side ("side-drape"), and dropping from the top ("plop"), shown in Fig. 2a. Examples of these tests and each of the approach trajectories are shown in the first supplemental video. These strategies were tested using a robot arm (UR5e, Universal Robots) with five grasp trials per strategy and object, with each object centered on a table below the gripper, and the results are shown in Figure 2b. Overall, the top-drape approach strategy had the highest success rate for both simple and complex objects, whereas all other approach strategies failed to grasp the three simplest objects. The side-drape did, however, outperform the other two trajectories in grasping the simple branched structures and could potentially compensate for centering errors.

Using the top-drape as the most broadly-successful method of approach, we evaluated the entanglement gripper's sensitivity to positioning errors following the methods used by Aukes et al. (34) and Sinatra et al. (22). Using a subset of objects (a sphere, cylinder, and branched structure), we performed grasps with controlled centering offsets in increments of 10mm, and measured the resulting grasp success rate over five trials at each location. The results of these experiments are shown in Figure 2c, as a function of the offset between center axis of the gripper and the center axis of the target object (normalized to the object radius) . Overall we found that complex objects are tolerant to large centering errors (see SI for additional tests and details). Our empirical investigation of grasping performance using non-deterministic entanglement is

particularly successful in grasping topologically and geometrically complex objects (10, 11) without the need for planning, but has trouble with simpler objects like spheres and vertical tubes where traditional deterministic grippers work well, e.g., the YCB object set of generally cylindrical, spherical, and cuboidal targets (35).

A secure grasp must be adaptive and strong. The collective softness of the entangled filaments provides the former. To characterize the strength of our gripper in the top-drape mode, we attached an object rigidly to the frame of an Instron universal testing machine and measured the gripper force or entanglement force opposing object pull-out. For the same gripper with 12 filaments and an operating pressure of $25psi$ ($172kPa$), the force-displacement curve was measured (see SI for details). We find that the maximum grasping forces achieved over the various objects was 27.6N, which is comparable to many robotic hands with soft, pneumatic fingers operating at similar pressures ( (17–20, 36)). While grip strength is a standard metric for robotic grippers, we propose that a more comprehensive metric is the toughness of a grasp - i.e. the energy required to break it. Grasp toughness is evaluated by the work done during a pull-out test, and scales with the bending energy to straighten the filaments, and also depends on the topological complexity of the target object and the level of entanglement. Values for the entangling 12-filament grasper tested in this work ranges from $10mJ$ for a $10cm$ sphere, to $380mJ$ for a simple branched structure, and $770mJ$ for a vertical $51mm$ cylinder. For comparison, values for the grasp toughness of recently developed soft grippers holding on to cylinders with diameters of $51 - 76mm$ are $200mJ$ (23), $300mJ$ (36), and $750mJ$ (18) (see SI for details).

To quantify the topological mechanics of robust grasping via collective filament entanglement, we now turn to a combination of scaling principles and numerical simulation. The characteristic curvature, $\kappa$, of an actuated filament subject to pressure $p$ scales as $\kappa \sim p(1-\delta)^2\epsilon/rE$ and follows from a simple torque balance (see SI for details). For grasping in the absence of gravity (e.g., in an aquatic environment), the radius of curvature of a filament $R \sim \kappa^{-1}$ must be smaller than the overall size of the target $R_T$ and furthermore the length of the filament, $l$ must satisfy $l \geq R_T$ to enable distributed contact. This is a conservative estimate, since in an array of filaments of areal density $\phi_G$, it may be possible to collectively entangle with the target since the effective curvature of a tangle will scale as $\kappa f(\phi_G)$ where $f(\phi_G) \geq 1$ is a function that depends on the

details of the filament array geometry. Therefore, a simple scaling relation for entanglement grasping via an array of long actuated filaments is given by $pR_T(1-\delta)^2\epsilon f(\phi_G)/rE \geq 1$. The former estimate ignores the effect of gravity and is thus valid in aquatic regimes. In terrestrial environments, an additional condition is that the weight of the target must be supported by the entanglement, so that $\rho_T R_T^4 g \leq Er^3 p(1-\delta)^2\epsilon f(\phi_G)$, a scaling result that follows from the balance between elastic and gravitational torques. These two scaling estimates characterize the geometric and mechanical requirements for grasping.

To go beyond these scaling ideas, we use numerical simulations of a director-based Cosserat continuum framework for slender filamentous objects (37–39) to explore the mechanics of rods capable of bend, twist, stretch, and shear deformation modes, all necessary to follow the geometrically nonlinear deformations of our elastomeric filamentous actuators. The governing nonlinear partial differential equations are a consequence of linear and angular momentum balance at each filament cross-section, taking into account internal force and torque resultants and external forces and torques (including inter-filament contact, friction from sliding contact, gravity, and internal viscous and external energy dissipation); these are then discretized and solved numerically (38, 39). The actuation of the filaments is replicated by introducing an intrinsic curvature everywhere along the length of the filaments at the instant of actuation, ignoring the dynamics of a propagating actuation scheme; this is tantamount to assuming that the actuated shape equilibrates fast relative to the dynamics of entanglement or contact creation with the target. In a gravitational field, where the filaments are straight and suspended from one end, upon actuation, the gripper filaments curl into helices, like hair, and make contact with other filaments and the target, leading to a soft entangled grasp. Although our simulation framework does not account for the effects of static friction or electrostatic forces due to charge build-up in sliding filaments, it is still capable of capturing the qualitative aspects of entanglement mediated grasping, replicating experimental observations (For details, see Supplemental Information), shown in Fig. 3a. We also show the ability of our simulation framework to tangle with and lift a branched structure using a top-drape as shown in Fig. 3a, remaining successful until the scaled offset is as large as $30\%$ of the target size, a conservative estimate given that we have not accounted for frictional effects in the simulations. A side-by-side comparison of the experimental and simulated grasps are shown in Fig. 3b as well as in the second supplementary video.

With the ability of the simulation to capture the topological and geometric complexity of entanglement grasping, we turn to explore the design space around the twelve-filament prototype gripper in terms of a phase space that spans the ratio of the target object spatial density $\phi_T$, the filament spatial density $\phi_G$, and a ratio of the density of the target object to that of the gripper. Examples of these trials with varying parameters are shown in Fig. 3d-f as well as their location on four planes of this phase space as shown in Fig. 3g-3j. Each point on these plots in Fig. 3g-f represents the results of seven trial runs of a simulated object grasp-and-pickup of an eight-branch structure like the one used in the physical testing (see SI for details). An individual trial was considered successful if the object was lifted off of the ground and remained suspended after 60s of the simulated time. The contour plot shows the success rate at the individual points and interpolates the predicted success rate between trial points using a Delaunay triangulation.

Secure grasping of an object in both animate (human) and inanimate (robotic) settings requires a characterization of the size, shape, mass distribution, and stiffness of the target, and suggests crucial roles for perception, planning, and action with feedback. Here we demonstrate that an embodied solution to this problem, relying on the flexible topology and geometry of the grasper leads to adaptable grasping without perception, planning, or feedback. We instantiate this flexible grasper using an array of slender, pneumatically actuated filaments that can entangle, wrap, or cradle target objects via distributed soft contacts. We deploy our entangling filament grasper to pick up targets with a range of sizes, topological complexities, geometric shapes, and mechanical flexibilities and characterize its performance in terms of phase diagrams. These diagrams are meant to be an initial exploration of the design space of hardware for entanglement grasping. A scaling and computational framework for entangling thin elastic filaments corroborates our experimental observations and phase diagrams. All together, our approach to the problem of robotic grasping complements traditional solutions using graspers with a few degrees of freedom but complex feedback control strategies, with infinite-dimensional graspers that are morphologically complex but without feedback. This ability to use complex morphology (geometry and topology) and dynamics (physics) and simple control rather than anthropomorphic morphology and complex control strategies will expand the range of objects conducive to robotic grasping but also enable us to understand how these solutions might have evolved in such examples as the elephant trunk or a jelly fish ambushing its prey (27, 40).

**Acknowledgments** This work was supported by a grant from the Office of Naval Research (Award #N00014-17-1- 2063), grants from the National Science Foundation (Awards #EFRI-1830901, #DMR-1922321, #DMR-2011754, and #EFMA-1830901), and by the National Science Foundation Graduate Research Fellowship (under Grants #DGE1144152 and #DGE1745303,), and the Wyss Institute for Biologically Inspired Engineering.

# References

1. M. T. Mason, *Annual Review of Control, Robotics, and Autonomous Systems* **1**, 1 (2018).

2. A. Bicchi, *IEEE Transactions on Robotics and Automation* **16**, 652–662 (2000).

3. M. R. Cutkosky, P. K. Wright, *The International Journal of Robotics Research* **5**, 20 (1986).

4. A. Bicchi, *The International Journal of Robotics Research* **14**, 319 (1995).

5. S. Jacobsen, E. Iversen, D. Knutti, R. Johnson, K. Biggers, *Proceedings. 1986 IEEE International Conference on Robotics and Automation* (IEEE, 1986), vol. 3, pp. 1520–1532.

6. W. Townsend, *Industrial Robot: an international journal* **27**, 181 (2000).

7. A. Kochan, *Industrial robot: an international journal* **32**, 15 (2005).

8. L. B. Bridgwater, *et al.*, *2012 IEEE International Conference on Robotics and Automation* (IEEE, 2012), pp. 3425–3430.

9. Robotiq, *Online datasheet* (2019).

10. J. Mahler, *et al.* (2017).

11. D. Morrison, P. Corke, J. Leitner, J. Leitner, *IEEE Robotics and Automation Letters* **5**, 4368 (2020).

12. L. U. Odhner, *et al.*, *The International Journal of Robotics Research* **33**, 736 (2014).

13. A. M. Dollar, R. D. Howe, *International Journal of Robotics Research* **29**, 585 (2010).

14. D. M. Aukes, *et al.*, *The International Journal of Robotics Research* **33**, 721 (2014).

15. W. Friedl, H. Höppner, F. Schmidt, M. A. Roa, M. Grebenstein, *2018 IEEE/RSJ International Conference on Intelligent Robots and Systems (IROS)* (IEEE, 2018), pp. 6469–6476.

16. M. G. Catalano, *et al.*, *The International Journal of Robotics Research* **33**, 768 (2014).

17. R. Deimel, O. Brock, *The International Journal of Robotics Research* **35**, 161 (2016).

18. K. C. Galloway, *et al.*, *Soft Robotics* **3**, soro.2015.0019 (2016).

19. J. Zhou, S. Chen, Z. Wang, *IEEE Robotics and Automation Letters* **2**, 2287 (2017).

20. J. Zhou, J. Yi, X. Chen, Z. Liu, Z. Wang, *IEEE Robotics and Automation Letters* **3**, 3379 (2018).

21. J. Zhou, *et al.*, *IEEE Access* **7**, 101483–101495 (2019).

22. N. R. Sinatra, *et al.*, *Science Robotics* **4** (2019).

23. S. Abondance, C. B. Teeple, R. J. Wood, *IEEE Robotics and Automation Letters* **5**, 5502 (2020).

24. P. Paoletti, G. Jones, L. Mahadevan, *Journal of the Royal Society Interface* **14**, 20160867 (2017).

25. J. Shintake, V. Cacucciolo, D. Floreano, H. Shea, *Advanced Materials* **30**, 1707035 (2018).

26. D. Rus, M. T. Tolley, *Nature* **521**, 467 (2015).

27. L. P. Madin, *Bulletin of Marine Science* **43**, 413 (1988).

28. K. P. Becker, Y. Chen, R. J. Wood, *Advanced Functional Materials* **30**, 2070075 (2020).

29. J. Paek, I. Cho, J. Kim, *Scientific Reports* **5**, 10768 (2015).

30. S. J. Gerbode, J. R. Puzey, A. G. McCormick, L. Mahadevan, *Science* **337**, 1087 (2012).

31. I. Must, E. Sinibaldi, B. Mazzolai, *Nature Communications* pp. 1–8 (2019).

32. K. Murasugi, *Knot Theory and Its Applications.*, Modern Birkhauser Classics (2008).

33. D. J. Montana, *IEEE Transactions on Robotics and Automation* **8**, 421 (1992).

34. D. M. Aukes, M. R. Cutkosky, *2013 IEEE International Conference on Robotics and Automation (ICRA)* pp. 2067–2073 (2013).

35. B. Calli, *et al.*, *IEEE Robotics & Automation Magazine* **22**, 36 (2015).

36. C. B. Teeple, T. N. Koutros, M. A. Graule, R. J. Wood, *The International Journal of Robotics Research* (2020).

37. E. Cosserat, F. Cosserat, *Théorie des corps déformables* (A. Hermann et fils,, 1909).

38. M. Gazzola, L. H. Dudte, A. G. Mccormick, L. Mahadevan, *Roy. Soc. Open Sci.* **5**, 171628 (2018).

39. N. Charles, M. Gazzola, L. Mahadevan, *Physical review letters* **123**, 208003 (2019).

40. R. Pfeifer, M. Lungarella, F. Iida, *science* **318**, 1088 (2007).

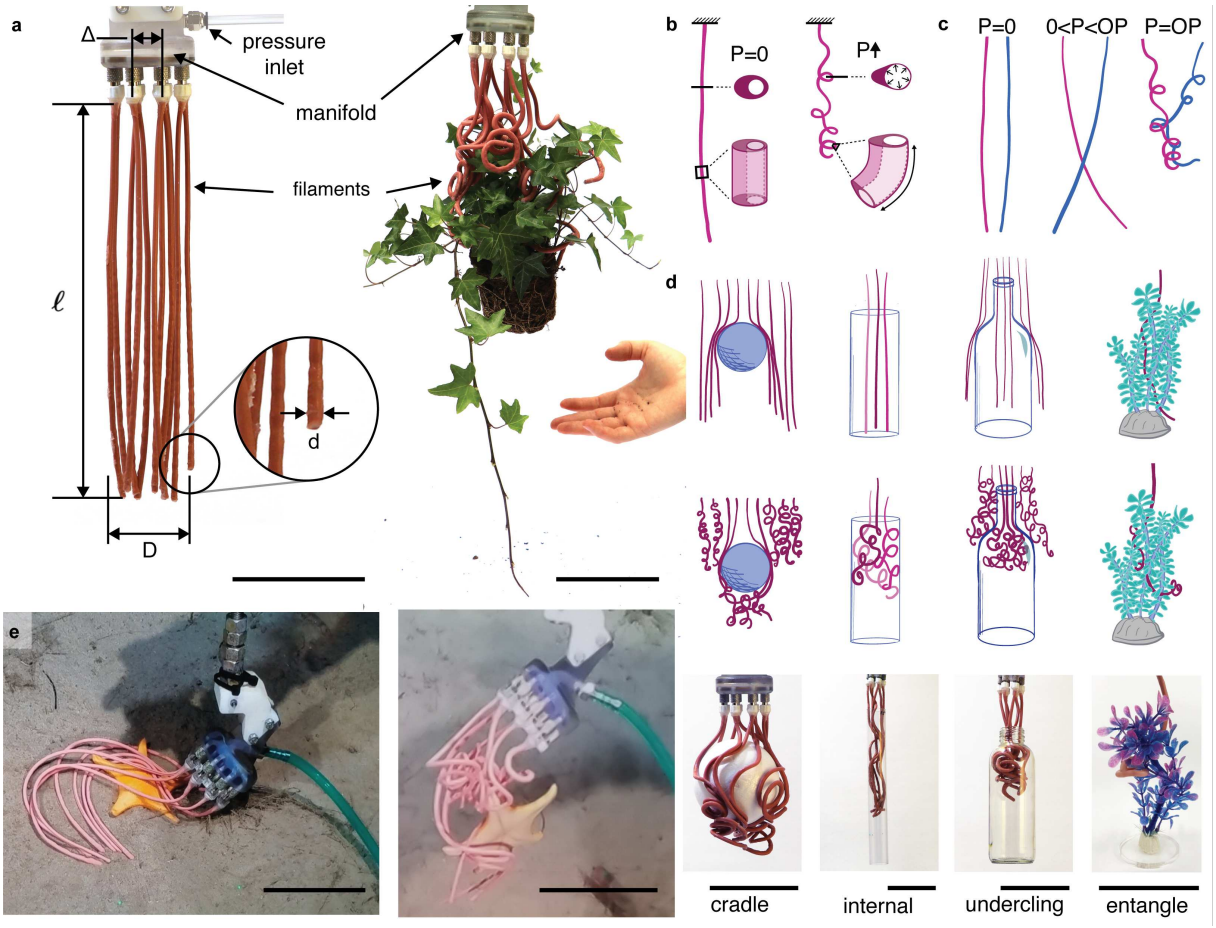


Figure 1: A) Picture of an entangling filament gripper consisting of 12 hollow elastomeric filaments in a resting state and pneumatically actuated around a house plant. B) Schematic of filaments at ambient and increased internal pressure. B) Schematic of filaments intertwining. Filaments start mostly straight when hanging under gravity, develop a slight curve at low pressure, and then snap to a tightly curled shape close to the operating pressure (OP). The operating pressure for the filaments shown in this work is approximately 25psi (172 kPa). D) The final shape of the actuated filaments and resulting grasp is affected by object interactions. The schematic shows unactuated and actuated states in the presence of a sphere, tube, bottle, and artificial plant. The photos show examples of physical tests with the same objects. E) Photos from a field test at 800m under water, demonstrating that the filaments can also be operated hydraulically and can operate under high hydrostatic pressure. The scale bars in the images represent 10cm.

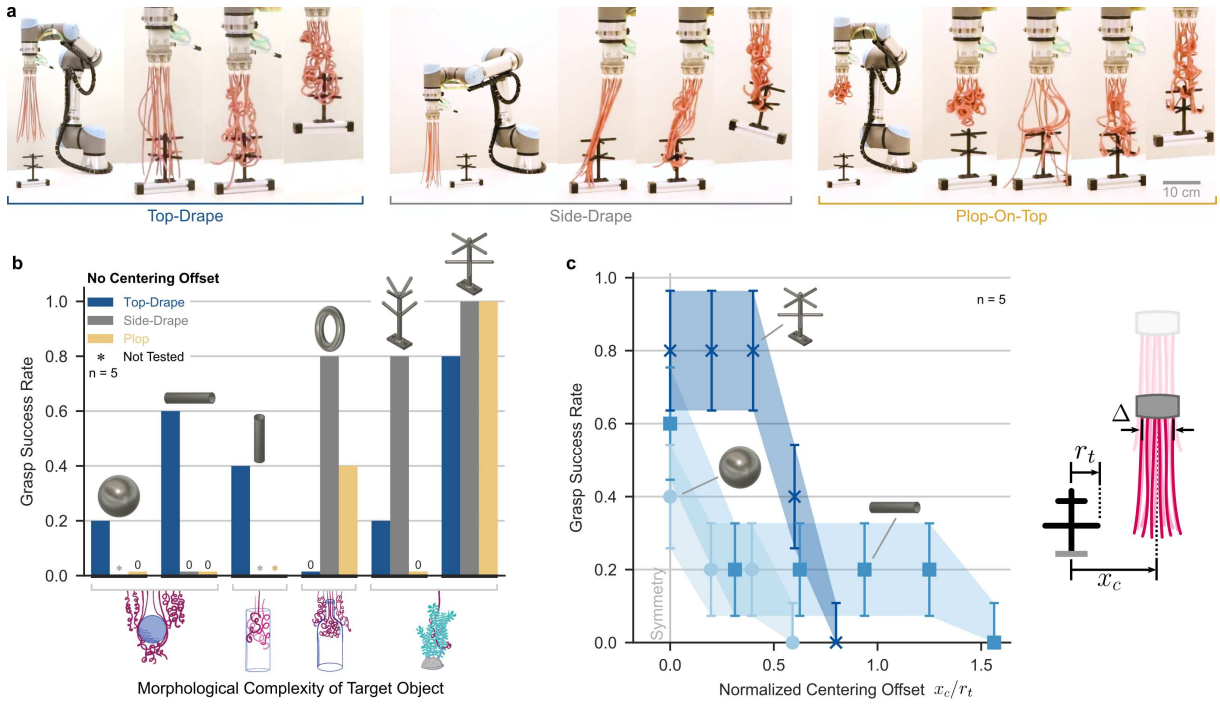


Figure 2: Three heuristic grasping approach trajectories were evaluated on objects of varying complexity. a) Typical pick-and-place operations with each of the three approach trajectories are shown, where the object's initial pose remains constant for all tests. b) Grasps on morphologically complex objects are very successful, particularly with a side-drape grasp. Conversely, the gripper has a lower success rate when attempting to grasp simple objects, with only a top-drape producing successful grasps for the three simplest objects. c) Top-drape grasps on complex objects are robust to centering errors up to $0.5\times$ the object diameter. The results of these experiments for an expanded set of objects and grasp approach motions can be found in the Supplementary Materials.

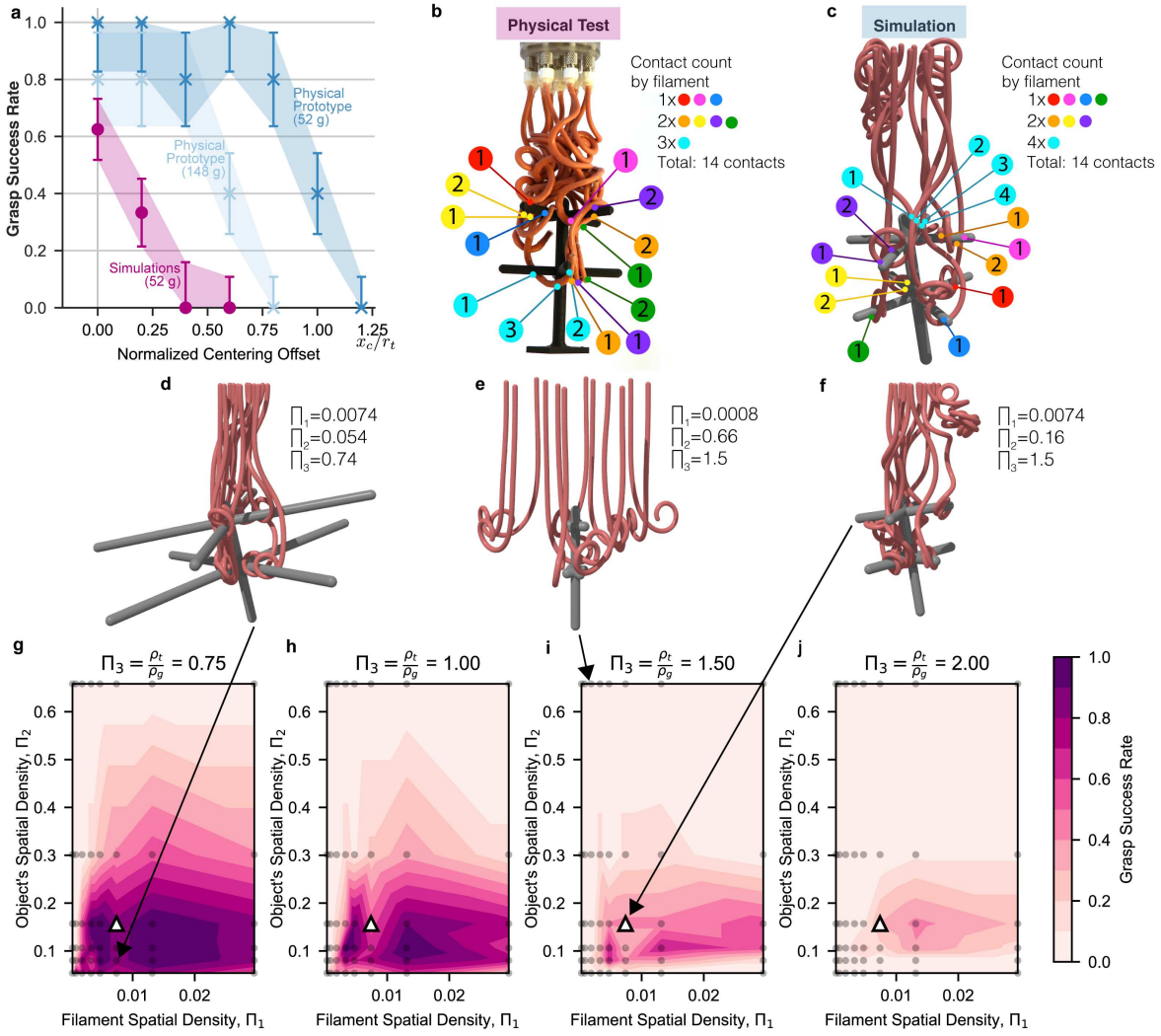


Figure 3: Results of the simulated entanglement performance compared with physical testing benchmarks. a) A plot of the experimental and simulated position error sensitivity while grasping a 52g eight-branch tree test object in comparison to the results presented in Figure 2C with a 148g eight-branch tree. b,c) Examples of contact distributions when the entanglement gripper holds an 52g eight-branch tree in a physical test (b) and simulated test (c). Contacts are indicated and sorted by the number of contacts made by unique filaments. In both of the examples shown, 14 contacts are made with eight unique filaments from an array of 12 filaments. d,e,f) Example simulated trials of vary target size, filament spacing, and object density. g,h,i,j) Success rates of simulated grasp tests assuming perfect centering over the eight-branch test object with varying gripper filament spacing, branch length, and four densities of the test object. The prototype and object parameters used in physical testing are indicated by the white triangle.

# Figures

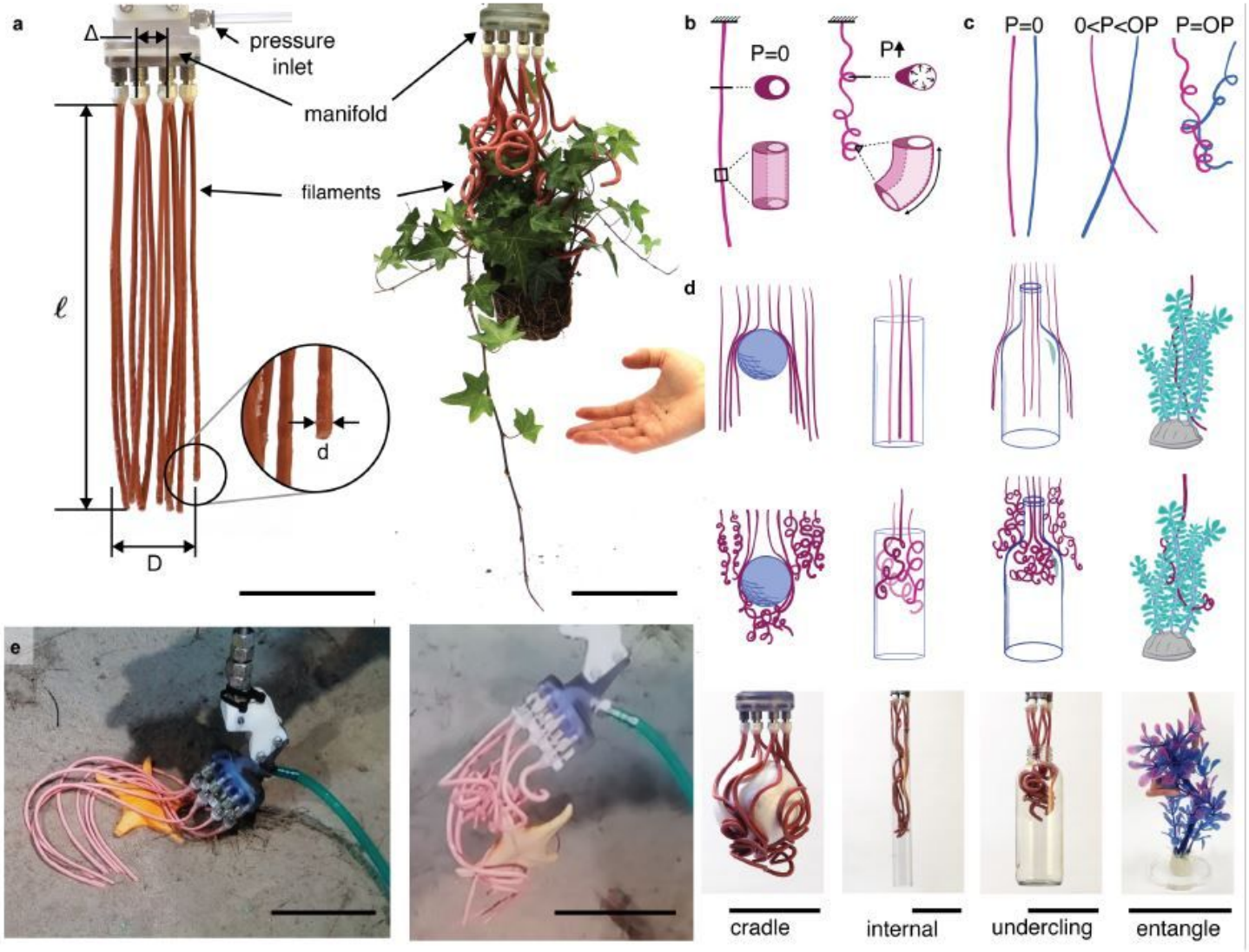


**Figure 1**

A) Picture of an entangling filament gripper consisting of 12 hollow elastomeric filaments in a resting state and pneumatically actuated around a house plant. B) Schematic of filaments at ambient and increased internal pressure. B) Schematic of filaments intertwining. Filaments start mostly straight when hanging under gravity, develop a slight curve at low pressure, and then snap to a tightly curled shape close to the operating pressure (OP). The operating pressure for the filaments shown in this work is approximately 25psi (172 kPa). D) The final shape of the actuated filaments and resulting grasp is affected by object interactions. The schematic shows unactuated and actuated states in the presence of a sphere, tube, bottle, and artificial plant. The photos show examples of physical tests with the same objects. E) Photos from a field test at 800m under water, demonstrating that the filaments can also be operated hydraulically and can operate under high hydrostatic pressure. The scale bars in the images represent 10cm.

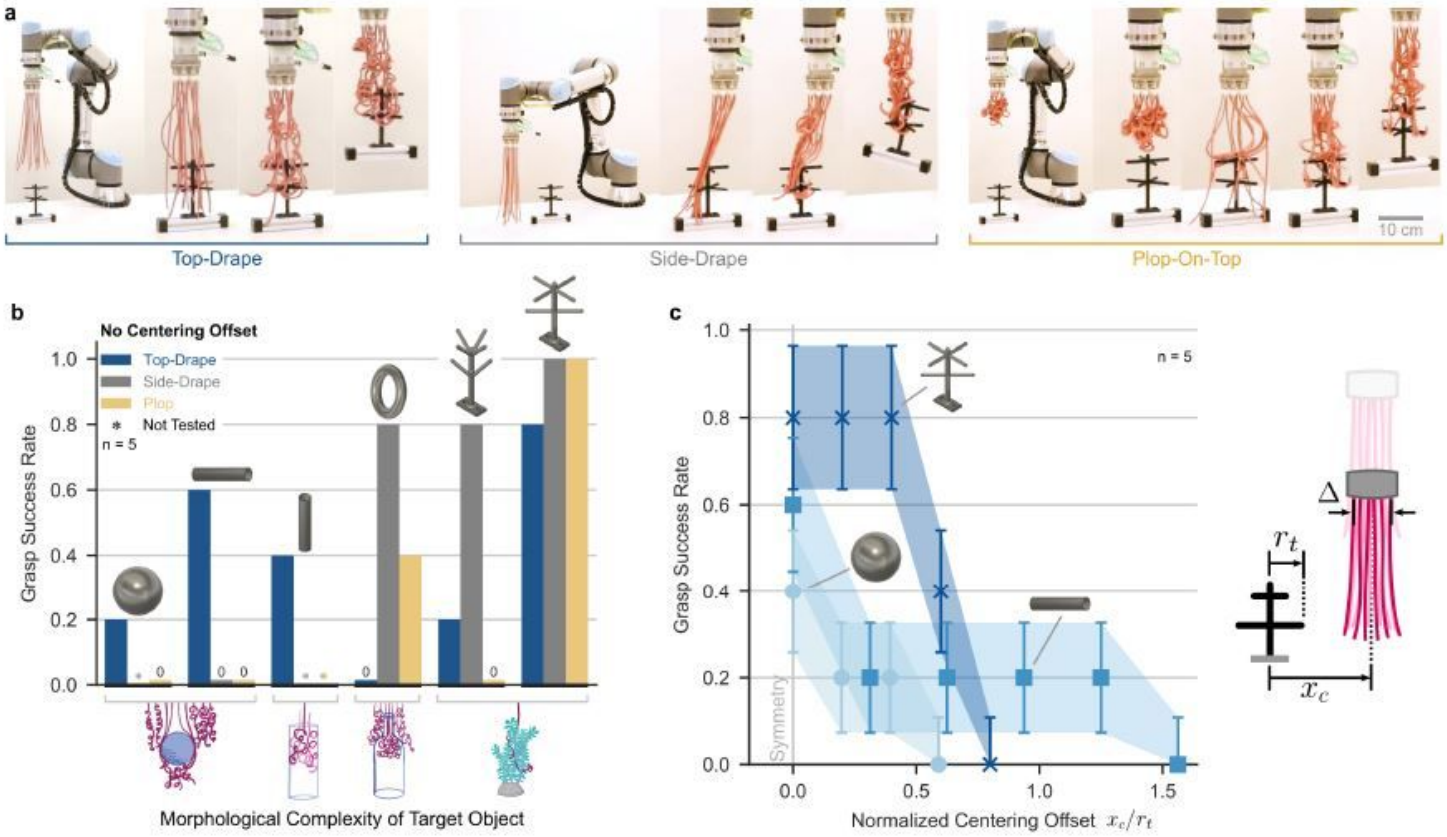


## Figure 2

Three heuristic grasping approach trajectories were evaluated on objects of varying complexity. a) Typical pick-and-place operations with each of the three approach trajectories are shown, where the object's initial pose remains constant for all tests. b) Grasps on morphologically complex objects are very successful, particularly with a side-drape grasp. Conversely, the gripper has a lower success rate when attempting to grasp simple objects, with only a top-drape producing successful grasps for the three simplest objects. c) Top-drape grasps on complex objects are robust to centering errors up to 0:5x the object diameter. The results of these experiments for an expanded set of objects and grasp approach motions can be found in the Supplementary Materials.

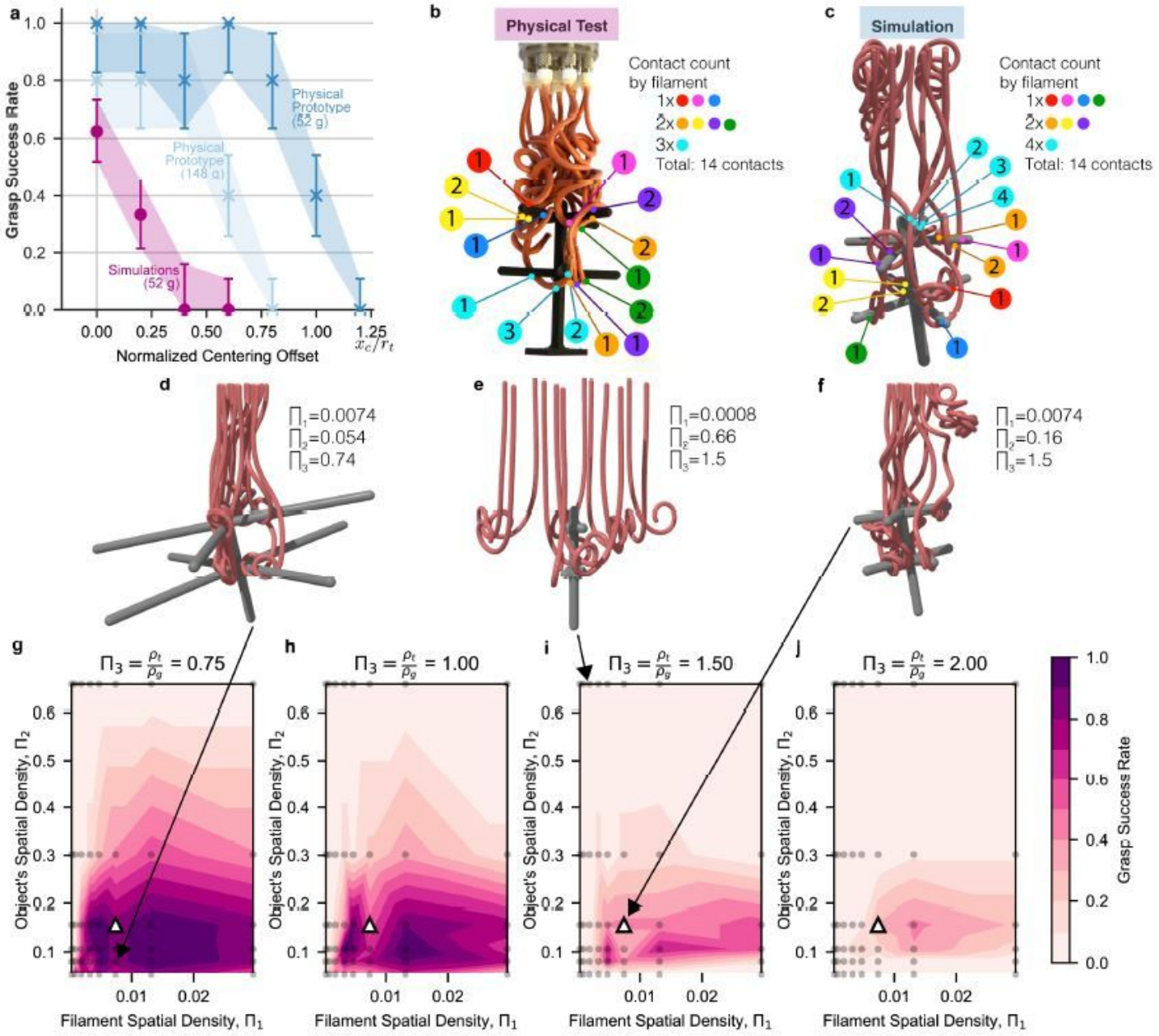


## Figure 3

Results of the simulated entanglement performance compared with physical testing benchmarks. a) A plot of the experimental and simulated position error sensitivity while grasping a 52g eight-branch tree test object in comparison to the results presented in Figure 2C with a 148g eight-branch tree. b,c) Examples of contact distributions when the entanglement gripper holds an 52g eight-branch tree in a physical test (b) and simulated test (c). Contacts are indicated and sorted by the number of contacts made by unique filaments. In both of the examples shown, 14 contacts are made with eight unique filaments from an array of 12 filaments. d,e,f) Example simulated trials of vary target size, filament spacing, and object density. g,h,i,j) Success rates of simulated grasp tests assuming perfect centering over the eight-branch test object with varying gripper filament spacing, branch length, and four densities

of the test object. The prototype and object parameters used in physical testing are indicated by the white triangle.

## Supplementary Files

This is a list of supplementary files associated with this preprint. Click to download.

- Video2simulations.mp4
- SupplementalText.pdf
- SupplementalText.pdf
- Video1PhysicalHardware.mp4